



A 4-pyridyltetrazole-based zinc metal-organic framework for photocatalytic degradation of methylene blue

Arti Chouhan^{*a}, Ashutosh Pandey^a, Sadhana Singh^b and Subia Ambreen^c^aDepartment of Chemistry, Motilal Nehru National Institute of Technology Allahabad, Prayagraj-211 004, Uttar Pradesh, India^bShri Ramswarop Memorial University, Lucknow-225 003, Uttar Pradesh, India^cDepartment of Applied Science and Humanities (Chemistry), Rajkiya Engineering College Bijnor, Bijnor-246 725, Uttar Pradesh, India

E-mail: artichouhan@mnnit.ac.in

Manuscript received online 10 July 2020, revised and accepted 31 October 2020

Metal organic frameworks (MOFs) have been found to be potentially effective for treatment of industrial wastewater. In the present work, a metal-organic framework [mono(5-(4-pyridyl)tetrazolato)hydroxylzinc(II)]monoaqua (**1**) has been synthesized and characterized. The average particle size of the product was calculated to be 43 nm by X-ray diffraction. In addition, the efficacy of the synthesized MOF as a photocatalyst was investigated by taking a common wastewater dye methylene blue (MB). The photocatalytic activity MOF (**1**) has been found to be 86% within one hour for 16 ppm of methylene blue (MB) dye using 0.8 g/L of catalyst.

Keywords: Metal-organic frameworks, industrial wastewater, photocatalyst, degradation, methylene blue.

Introduction

Metal organic frameworks (MOFs) are synthesized by the systematic joining of metal centres and organic ligands, resulting in crystalline and porous materials¹. MOFs based on tetrazole ligands are a comparatively new class in coordination polymers due to a vast structural range and interesting topologies². The tunable structures of MOFs via careful selections of metal ions and organic moieties, make them attractive for various applications like adsorption, water harvesting, gas storage, gas separation, drug delivery, catalysis and sensing³⁻⁵ etc. Like structural tunability, the optical characteristics of MOFs can also be controlled by the correct choice of organic ligand and metal ion, and they can be conveniently used as photocatalyst^{6,7}. These types of catalytic activities are quite common for degradation of organic dyes in case of metal oxides⁸ but are relatively new fields of research in MOFs. Recently, significant efforts have been made to develop highly crystalline porous MOF materials for industrial wastewater treatment⁹. These materials demonstrate excellent chemical stability under extremely acidic

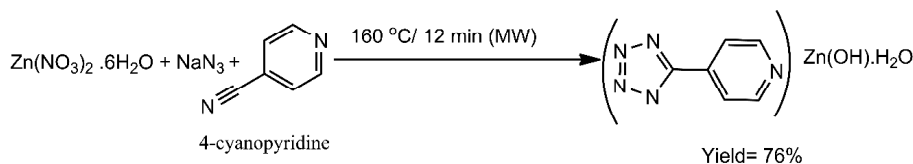
conditions that exhibit significant photocatalytic CO₂ reduction under visible light¹⁰. Furthermore, we have also reported¹¹⁻¹³ few MOFs that had elongated morphology (tube/needle rod-shaped) with better porosity and induced properties.

In this paper, we discussed the synthesis of a MOF, [Zn(OH)(4-PTZ).H₂O]¹⁴ (**1**), using fast and facile microwave assisted solvothermal method through *in situ* [2+3] cyclic addition of -CN and -N₃ groups (Scheme 1). As synthesized hexagonal rod-shaped MOF compound has been characterized through Fourier transform infrared spectroscopy, X-ray powder diffraction (XRPD), scanning electron microscopy, surface area analysis, and photoluminescence. Also, the photocatalytic decomposition of the methylene blue (MB) dye has also been investigated using UV-Visible spectrophotometer.

Experimental

Materials and methods:

Zn(NO₃)₂.6H₂O, 4-pyridine carbonitrile and NaN₃ were



Scheme 1. Synthesis of compound (1).

purchased from Sigma-Aldrich, India. The RIGAKU Smartlab X-ray diffractometer using Cu K α (X-ray wavelength (λ) for K α = 1.54 Å) was used for calculating the crystal size and for structure confirmation. Morphology of the synthesized MOF compound was determined using SEM of Zeiss EVO MA 15 make. Surface area investigation was carried out using Smart Sorb 93-surface area analyzer.

Method for synthesis of MOF (1):

The measured amounts of Zn(NO₃)₂·6H₂O (1 mmol), 4-pyridinecarbonitrile (2 mmol) and sodium azide (3 mmol) were dissolved in 10 ml double distilled water and 3 ml dimethylformamide. Subsequently, the sample was heated in a microwave oven at 160°C for 12 min and kept to cool to room temperature (RT). Lastly, washed powdered crystals of compound (1) were collected after drying in an electric oven for 6 h at 60°C. Elemental analysis (%) Calcd. for ZnC₆N₅H₇O₂: C, 29.21; H, 2.79; N, 28.38. Observed for (1) (%): C, 28.88; H, 2.29; N, 28.42.

Photocatalytic experiment:

For photocatalytic activity test, a light source with a wavelength range 200 to 600 nm having a maximum intensity at a wavelength of 365 nm was used. The photocatalysts in specific amounts (0.8 mg/mL) were dispersed in 5×10⁻⁵ mol L⁻¹ of MB aqueous solution. Subsequently, two drops of 30% H₂O₂ solution was added to the solution. For one-hour adsorption-desorption was maintained to achieve equilibrium in the dark. 1 mL of the suspension was taken at fixed intervals of 10 min for analysis. UV-Vis spectrophotometer was used to record the absorption spectrum for determining the residual MB concentration at 650 nm.

Results and discussion

In the IR spectrum (Fig. 1), presence of a broad band at 3400–3500 cm⁻¹ shows that coordinated water molecule is present in the compound. The presence of peaks in series 1657–1447 cm⁻¹ shows the occurrence of [2+3] cyclization reaction between -CN and -N₃ groups.

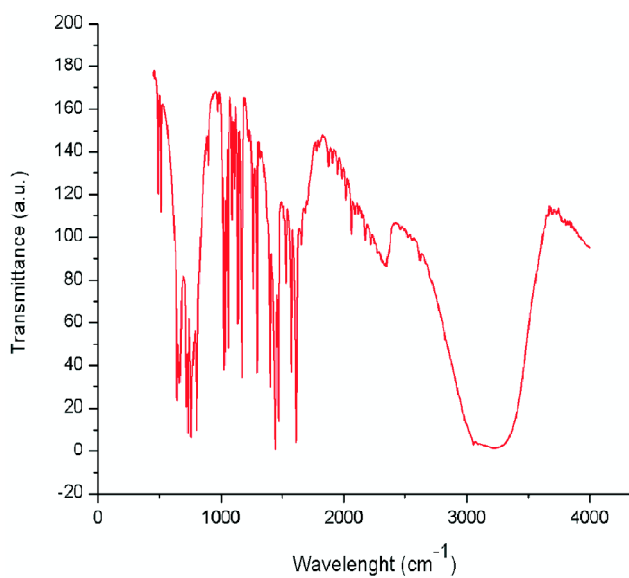


Fig. 1. The IR spectrum of compound (1).

The structure of Zn(OH)(4-PTZ)·H₂O was analyzed and confirmed by matching XRPD pattern against the simulated pattern of the single crystal structure¹⁴ of Zn(OH)(4-PTZ)·H₂O. From the XRPD pattern, it was found that compound (1) was formed without any impurities (Fig. 2). The characteristic peaks are designated to be (002), (102), (202), (300), (212), (204), (020), (122) and (124). The average crystallite size of compound (1) was calculated using Debby-Scherer equation which was 43 nm. The SEM image depicting the elongated hexagonal rod-shaped morphology of the synthesized microcrystals is shown in Fig. 3. The micrometric hexagonal rods of 10–15 μm in length and 1–2 μm in width are clearly visible in image. From the BET technique, the specific surface area of compound (1) was found to be 54 m²/g.

Subsequently, photoluminescent property of compound (1) has been examined at RT (Fig. 4). After irradiation of 360 nm of ultraviolet light, the maximum wavelength of the emission spectrum observed was 390 nm. The emission peak in

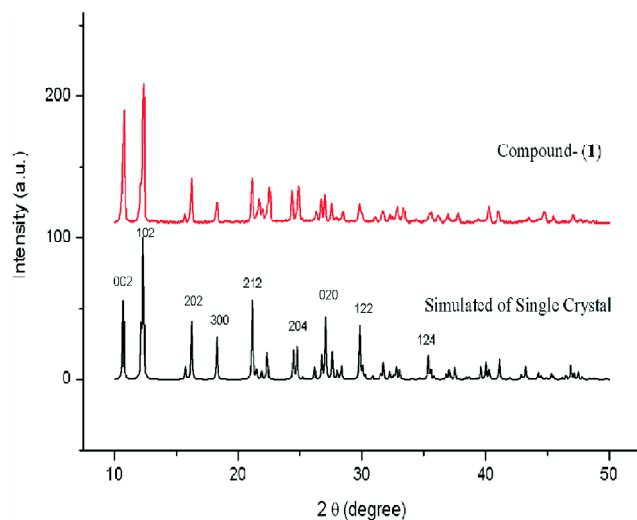


Fig. 2. Comparison of XRPD patterns of synthesized compound (1) with the simulated data of single crystal¹⁴.

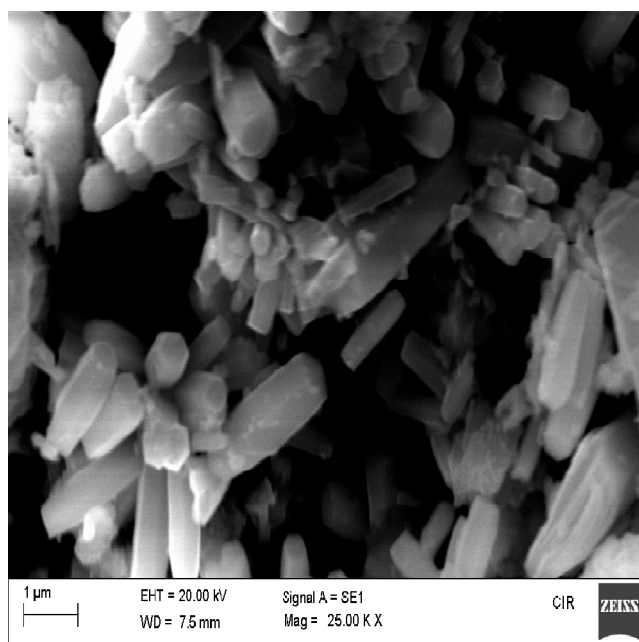


Fig. 3. SEM image of compound (1).

compound (1) is occurring due to $5s_{Cd} \rightarrow \pi_{Lz}$ metal-to-ligand charge transfer transition. In UV-Vis absorption spectrum a broad absorption band centred on 353 nm (λ_{max}) can be seen, which is apparently due to the optical transition of ligand-to-metal charge transfer (Fig. 5). The bandgap value at 3.13 eV is obtained from the same λ_{max} , calculated using Tauc plot (Fig. 5 (inset)).

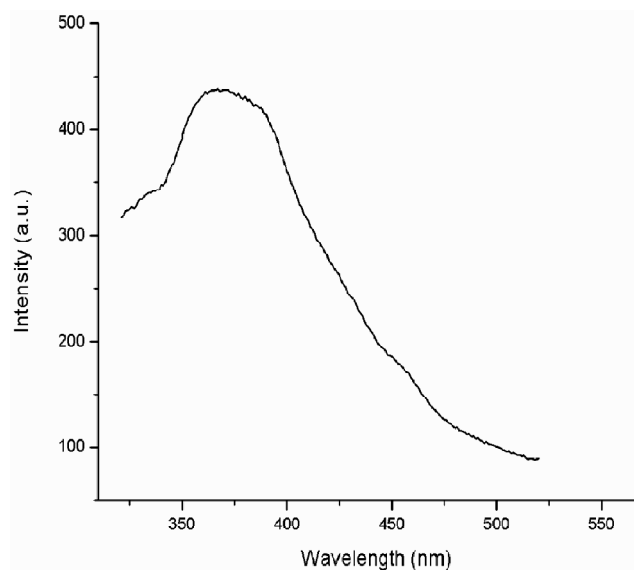


Fig. 4. The emission spectrum of compound (1) at room temperature.

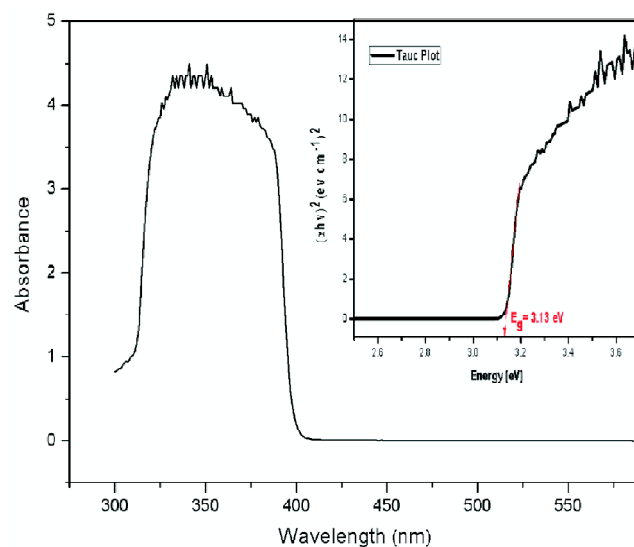


Fig. 5. UV-Vis absorption spectrum of compound (1). The Tauc plot is shown in inset.

The photocatalytic activities of MOF (1) and Degussa P-25 (as a reference photocatalyst) put together in Fig. 6. Experimental details have already been given in the Experimental Section. It is quite notable that the addition of a small quantity of H_2O_2 as an oxidant significantly improves the activity of the photocatalyst. The photocatalytic reaction was initiated with the generation of electron-hole pairs. Here the improved photodegradation efficacy can be described by

Table 1. Summary of results of MOF (1)

| MOF Sample | Synthesis time (min) | Porosity (m ² /g) | Crystallite size (nm) | Band-gap Value (eV) | [MB] ₀ (ppm) | R/60 Min (%) | k (min ⁻¹) |
|------------|----------------------|------------------------------|-----------------------|---------------------|-------------------------|--------------|------------------------|
| Rod-shaped | 12 | 54 | 43 | 3.13 | 16 | 86 | 0.0231 |

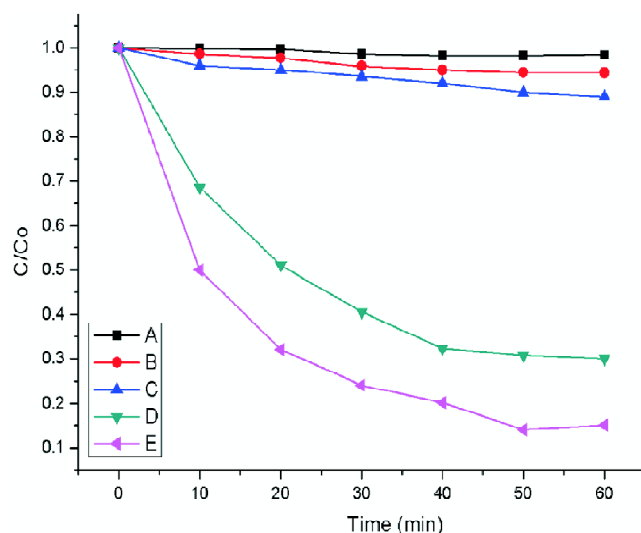


Fig. 6. Photocatalytic activity of Zn-MOF photocatalyst: [— —A] Dye/without photocatalyst in light, [— —B] Dye/photocatalyst in dark, [— —C] Dye/without photocatalyst/with H₂O₂ in light, [— —D] Dye/P-25/H₂O₂ under radiations, [— —E] Dye/photocatalyst/H₂O₂ under radiations.

equation ($\text{H}_2\text{O}_2 + e^- \rightarrow \text{OH}^- + \cdot\text{OH}$)¹¹. For the given time of 60 min, degradation of MB using (1), degradation of MB using Degussa P-25 (as a reference photocatalyst) and degradation of MB without using (1) were found to be 86%, 70% and 11% respectively. Fig. 7 shows the scatter plots of $\ln(C_0/C)$ versus irradiation time (min) for different reactions along with their linearly fitted trend-lines. Value as given in brackets of the legends is the rate of degradation k (min⁻¹). This indicates that good photocatalytic activity was achieved for MOF (1), due to its small average crystallite size, elongated shape, optimum surface area, and judicious band gap^{11,12}. In addition, a diverse structure with an elevated aspect ratio contributes to ballistic photo-generated carrier transport and propagates charge across longitudinal lengths¹⁵. Some studies have reported that ballistic charge transfer in the range of one-dimensional structures is much more useful than higher dimensions¹⁶. This may be the reason for good decomposition rate of MB dye with a micrometric hexagonal rod-like photocatalyst.

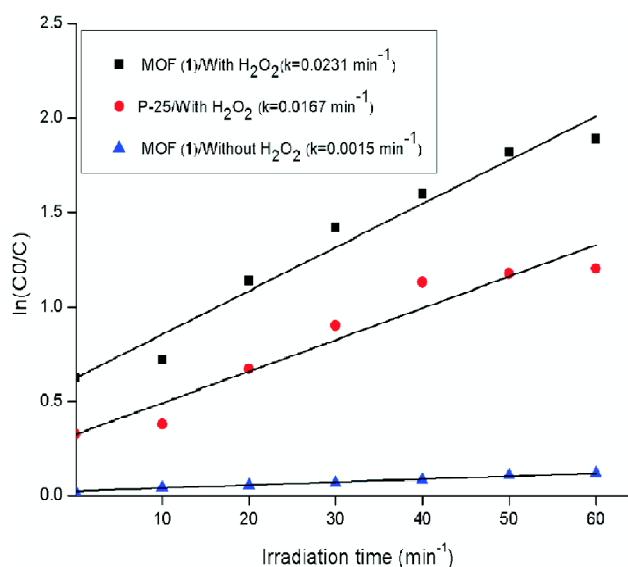


Fig. 7. Graphical determination of reaction rate of the photocatalytic degradation of MB by [— —] MOF (1)/with H₂O₂ ($k = 0.0231 \text{ min}^{-1}$), [— —] P-25/with H₂O₂ ($k = 0.0167 \text{ min}^{-1}$), [— —] MOF (1)/without H₂O₂ ($k = 0.0015 \text{ min}^{-1}$).

Conclusions

The synthesis, characterisation, morphological property and photocatalytic activity of MOF based on 4-pyridyltetrazole ligand are discussed. MOF (1) was synthesized using the microwave assisted solvothermal technique in a lesser reaction time (12 min) than the traditional hydro/solvothermal method (1 to several days). Upon studying the photocatalytic property of the sample, it has been observed that MOF (1) is a good candidate for photocatalytic degradation of organic dyes. This approach is expected to be widely used in large scale production of MOFs.

Acknowledgements

Arti Chouhan gratefully acknowledged the DST, Government of India for taking financial assistance under the Women's Scientific Scheme (WOS-A). Authors thanked center for interdisciplinary research (CIR) of MNNIT, Allahabad.

References

1. S. Rojas and P. Horcajada, *Chem. Rev.*, 2020, **120**, 16, 8378.
2. E. A. Popova, R. E. Trifonov and V. A. Ostrovskii, *ARKIVOC*, 2012, **1**, 45.
3. R. Haldar, S. Bhattacharyya and T. K. Maji, *J. Chem. Sci.*, 2020, **132**, 1.
4. A. Terzopoulou, J. D. Nicholas, X. Z. Chen, B. J. Nelson, S. Pane and J. P. Luis, *Chem. Rev.*, 2020, **120**, 20, 11175.
5. B. M. Connolly, M. Aragoes-Anglada, J. Gandara-Loe, N. A. Danaf, D. C. Lamb, J. P. Mehta and A. E. Wheatley, *Nat. Commun.*, 2019, **10**, 1.
6. Q. Wang, Q. Gao, A. M. Enizi, A. Nafady and A. Ma, *Inorg. Chem. Front.*, 2020, **7**, 300.
7. H. Furukawa, K. E. Cordova, M. O'Keeffe and O. M. Yaghi, *Science*, 2013, **341**, 1230444.
8. D. K. Bhole, R. G. Puri, P. D. Meshram and R. S. Sirsam, *J. Indian Chem. Soc.*, 2020, **97**, 440.
9. M. Priyadarshini, I. Das and M. M. Ghangrekar, *J. Indian Chem. Soc.*, 2020, **97**, 507.
10. S. Wang, T. Kitao, N. Guillou, M. Wahiduzzaman, C. Martineau-Corcos, F. Nouar and S. Kitagawa, *Nat. Commun.*, 2018, **9**, 1660.
11. A. Chouhan, G. Pilet, S. Daniele and A. Pandey, *Chin. J. Chem.*, 2017, **35**, 209.
12. A. Chouhan, P. Mayer and A. Pandey, *Indian J. Chem.*, 2015, **54A**, 851.
13. A. Chouhan, A. Pandey and P. Mayer, *J. Chem. Sci.*, 2015, **127**, 1599.
14. L. Z. Wang, Z. R. Qu, H. Zhao, X. S. Wang, R. G. Xiong and Z. L. Xue, *Inorg. Chem.*, 2003, **42**, 3969.
15. C. W. J. Beenakker and H. Houten, *Solid State Phys.*, 1991, **44**, 1.
16. D. Jiang, P. Xu, H. Wang, G. Zeng, D. Huang, M. Chen, C. Lai, C. Zhang, J. Wan and W. Xue, *Coord. Chem. Rev.*, 2018, **376**, 449.